Isotope Effects on the Phase Separation in Polystyrene–Poly(vinyl methyl ether) Blends. 2. Influence of the Microstructure of Linear and Star Block Copolymers

J. M. Gomez-Elvira,† J. L. Halary,* and L. Monnerie

Laboratoire de Physicochimie Structurale et Macromoléculaire, Ecole Supérieure de Physique et Chimie Industrielles de la Ville de Paris, F-75231 Paris Cedex 05, France

L. J. Fetters

Corporate Research Laboratories, Exxon Research and Engineering Company, Annandale, New Jersey 08801

Received May 13, 1993; Revised Manuscript Received February 3, 1994®

ABSTRACT: Phase separation trends in blends of poly(vinyl methyl ether) (PVME) with various hydrogenous block-deuterated polystyrenes (PS) have been studied by a fluorescence technique. In the case of linear polystyrenes of a given overall chain length and deuterium content, the position of the LCST-type phase diagrams in the temperature–composition plane is shown to depend on whether the deuterated block is located in the middle or at the end of the chain. Additionally, it is observed that the kinetics of spinodal decomposition differ from one system to the other. The inspection of the phase behavior of mixtures, including star-shaped hydrogenous-block-deuterated PS's, and the investigation of the solubility properties of the PS copolymers in a monomeric analog of PVME support the idea that the polymer–polymer interaction parameter depends on copolymer morphology, namely, on the accessibility of the ether functions to the thermodynamically-favored deuterated phenyl rings of polystyrene.

Introduction

The pair polystyrene (PS)–poly(vinyl methyl ether) (PVME) has played a prominent role as a model system of thermally-induced phase separation in polymer blends. A number of experimental techniques have been used in these investigations. Early studies revealed the influence of polymer molecular weight,[1,2] polydispersity,[3] and isotope substitution on the location of the phase diagram (and mainly of its minimum, the so-called LCST) in the temperature–composition plane. Regarding the effect of PS deuteration, evidence was produced from cloud point measurements[4] and then from fluorescence and small-angle neutron scattering experiments[5] that the use of perdeuterated PS (PS-d_8) instead of hydrogenous PS (PSH) of identical chain length leads to an increase in the LCST by about 40 °C. Later, it was shown[3] that blends of PVME with poly(1-pentadeuteriophenyl)ethylene (PS-d_5) exhibit phase diagrams comparable to those of PVME blended with perdeuterated PS-d_8 whereas blends of PVME with poly(1-phenyltrideuterioethylene) (PS-d_3) and PVME with PSH behave similarly. These observations confirm that the interactions of PVME with the deuterated phenyl rings of PS are thermodynamically favored. Finally, inspection of PVME–PSH–PS-d_8 ternary blends revealed a progressive increase in LCST with PS-d_8 content, which has been interpreted in terms of preferential solvation of PVME by the deuterated chains.[5]

In an attempt to improve our understanding of these isotope effects, this paper investigates the phase behavior of blends of PVME with some PS block copolymers consisting of hydrogenous and perdeuterated sequences. As sketched in Figure 1, four materials are analyzed in this study, namely, a diblock copolymer (PS-HD), a triblock copolymer (PS-HDH), and two 6-arm star-shaped PS's whose center is either hydrogenous (PS-$(HD)_6$) or perdeuterated (PS-$(DH)_6$).

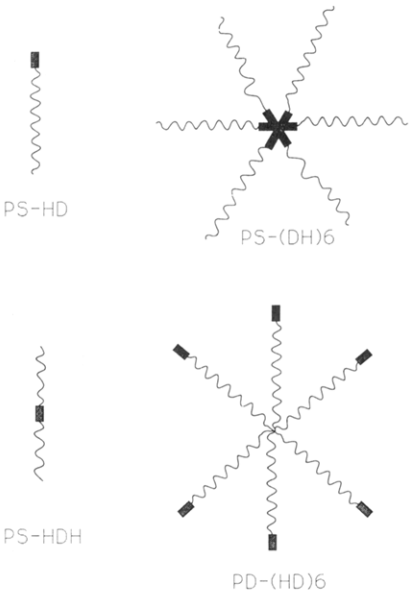

Figure 1. Schematic representation of the PS's: (〰) hydrogenous block; (■) deuterated block.

As in our previous studies,[1-3,5] the fluorimetric method described in ref 6 was used to determine the phase diagrams. The sensitivity of this technique has proven to be greater than that of light scattering measurements and comparable to that of small-angle neutron scattering.[5] In addition, this technique is capable of providing information on the kinetics of phase separation.[7]

Experimental Section

Materials. The origin and molecular weight characteristics of the polymer samples are given in Table 1. They have been extensively studied in the past in the view of their relaxation properties;[8] for this purpose, they were carefully characterized by steric exclusion chromatography and were shown to be free from homopolymer contaminant.

PS* is the designation of the hydrogenous PS chains which include one anthracene moiety in their middle. They are used

* To whom correspondence should be addressed.
† Permanent address: Instituto de Ciencia y Tecnologia de Polimeros, E-28006 Madrid, Spain.
® Abstract published in *Advance ACS Abstracts,* April 15, 1994.

0024-9297/94/2227-3370$04.50/0

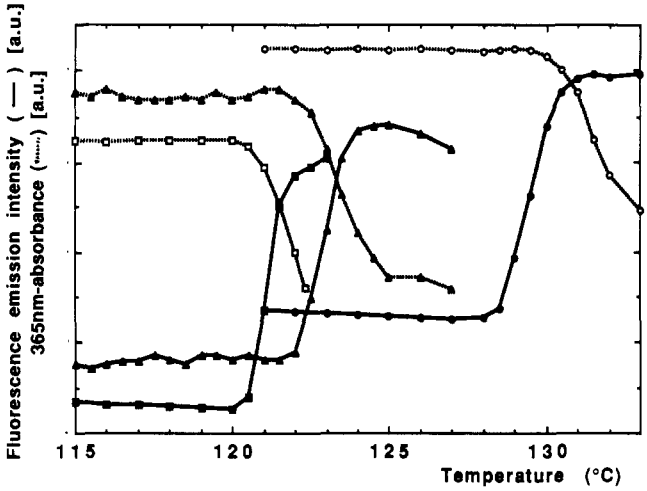

Figure 2. Fluorescence intensity (solid lines) and absorbance (dotted lines) versus temperature recorded during ramp experiments at 0.2 °C/min: squares, blend PVME/PSH (80:20); triangles, blend PVME/PS-HD (80:20); circles, blend PVME/PS-HDH (80:20).

Table 1. Polymer Origin and Characteristics

material design	origin	total mol wt M_n	total mol wt M_w	individual block mol wt (M_w) hydrogenous block	individual block mol wt (M_w) deuterated block
PVME	SP2	46 500	99 000		
PS-HD	Fetters[8]	175 000	184 000	157 000	27 000
PS-HDH	Fetters[8]	179 000	188 000	79 000	30 000
PS-(HD)$_6$	Fetters[8]	1 285 000	1 350 000	188 000	37 000
PS-(DH)$_6$	Fetters[8]	1 405 000	1 470 000	215 000	30 500
PSH	Fetters[8]	176 000	182 000		
PS*	Halary[1]	56 000	60 000		

as the fluorescent label and are incorporated in the blends in small amounts, typically 0.3%.

n-Butyl methyl ether (BME) and *tert*-butyl methyl ether (TBME), used in this study as monomeric analogs of PVME, were purchased from Aldrich.

Blend Preparation. Appropriate amounts of dried PVME and hydrogenated-block-deuterated PS (15 g of polymer/100 cm^3) were dissolved in a solution of PS* in benzene. The PVME/PS weight ratio was varied in the range 0.1–0.9. Next, films were cast on glass plates from the solutions and then dried in an oven at room temperature for 24 h followed by 24 h under vacuum and finally for 24 h at 60 °C under vacuum. It was verified that complete removal of the solvent had occurred under such drying conditions for all blend compositions. Typical thickness of the dried films was around 60 μm.

Cloud Point Measurements. Changes in the opacity of the PVME–PS blends during the phase separation process was followed under a fluorescence microscope illuminated at 365 ± 15 nm. Use of appropriate analysis filters allowed measurement of the light intensity transmitted at the excitation wavelength, without any artifact due to fluorescence emission. Appearance of the cloud point was detected by a rapid decrease of transmitted light intensity.

Low-temperature cloud points of solutions of the different PS's in mixtures of TBME and BME (3:1, 1.5:1, 1:1, and 1:1.5 volume ratios) were evaluated by eye. Polymer solutions in the concentration range 2–50 g L^{-1} were prepared in sealed tubes and left to homogenize at 27 °C inside a thermocryostat. Then they were cooled to different temperatures in the range +25 to −25 °C until cloudy. The cooling rate was around 10 °C/h.

Fluorescence Measurements. Measurements were carried out under continuous illumination using a fluorescence microscope with excitation and fluorescence emission wavelengths around 365 and 440 nm, respectively. As detailed in ref 7, phase separation is detected in the form of an upturn in fluorescence intensity. Some experiments were performed in a Mettler hot stage attached to the microscope under continuous heating at a rate ranging from 0.2 to 16 °C min^{-1}. Other experiments were carried out in the hot stage also, but under isothermal conditions. Thus, the equilibrium phase transition temperature, T_{coex}, was conventionally defined as the temperature at which the change in fluorescence intensity is as small as detectable over a 30-min period. Measurements of T_{coex} were reproducible to within ±0.5 °C.

Figure 2 shows the suitability of our hydrogenous PS* probe for detecting phase separation in the presence of hydrogenous-block-deuterated materials. Indeed, the fluorescence phase separation temperature, T_F, is systematically very close to the cloud point phase separation temperature, T_{CP}. This is the case whatever the degree of deuteration of the PS. As expected, T_F is a little smaller than T_{CP} as the result of the detection of earlier stages of phase separation.

For analysis of phase separation kinetics, samples were heated very rapidly in the hot stage up to temperatures of $T = T_{coex} + \Delta T$ and then held in isothermal conditions. The depth of quench, ΔT, ranged from 0.5 to 5.5 °C. Fluorescence intensity, I_F, was recorded continuously during the experiments. Initial rates of phase separation were derived from the plots of I_F versus time according to the procedure described in a previous publication.[7] As illustrated in Figure 3, the method involves, at any ΔT, (i) determination of the relative increase in fluorescence intensity, $\Delta I_{F\infty}$, from the initial one-phase state up to the plateau value (Figure 3a), (ii) plotting of the ratio $\Delta I_F/\Delta I_{F\infty}$ as a function of time, which represents the percentage of phase separation that has already occurred (Figure 3b), (iii) calculation, at any time, of the separation rates, v, from the slopes of the curves 3b, and (iv) determination of the initial phase separation rate, v_0, from the y intercept of the plot of $v(t)$ versus time (Figure 3c).

Results

In this section, we will consider first the linear block copolymers PS-HD and PS-HDH. Location of their phase diagrams in the presence of PVME and kinetics of phase separation are given and compared with the phase behavior of PVME/PSH and PVME/PS-d_8 blends of similar chain length. In addition, the UCST behavior of their solutions with BME and TBME is investigated. Second, we will present the data relative to the star PS's. These are preliminary results due to the absence, at the moment, of homologous hydrogenous and perdeuterated materials.

Linear PS-Based Blends. The phase coexistence curve of the blend PVME/PS-HD is compared in Figure 4 with those relative to the blends PVME/PSH and PVME/PS-d_8. The minima of these phase diagrams, characterized by the so-called T_{min} temperatures, obviously occur at the same critical weight fraction of PS, since the three PS's under consideration are of the same molecular weight and polydispersity. The T_{min} of PVME/PS-HD, detected at 128 ± 0.5 °C, is located between the values relative to PVME/PSH and PVME/PS-d_8, which are 120 ± 0.5 and 159 ± 0.5 °C, respectively. In the case of the blend PVME/PS-HDH, the phase coexistence curve (Figure 5) is also located in an intermediate position between PSH and PS-d_8, but much closer to PSH. The LCST, indeed, is observed at T_{min} = 121.5 ± 0.5 °C. The approximation of identical molecular weight for the different samples under comparison is supported by the weak molecular weight dependence of T_{min}: according to the linear relationship evidenced between T_{min} and $(\bar{M}_w)^{-1/2}$ in ref 2, a change in molecular weight of 2% in this range would result in a deviation of T_{min} as low as 0.2 °C, i.e., well below the experimental uncertainties on T_{min} determination. Thus, it is clear that, at identical overall chain length and deuterium content, the value of the LCST depends on whether the deuterated block is located in the middle or at the end of the PS chains.

Further analysis of the LCST values of the PVME/PS-HD and PVME/PS-HDH blends can be carried out

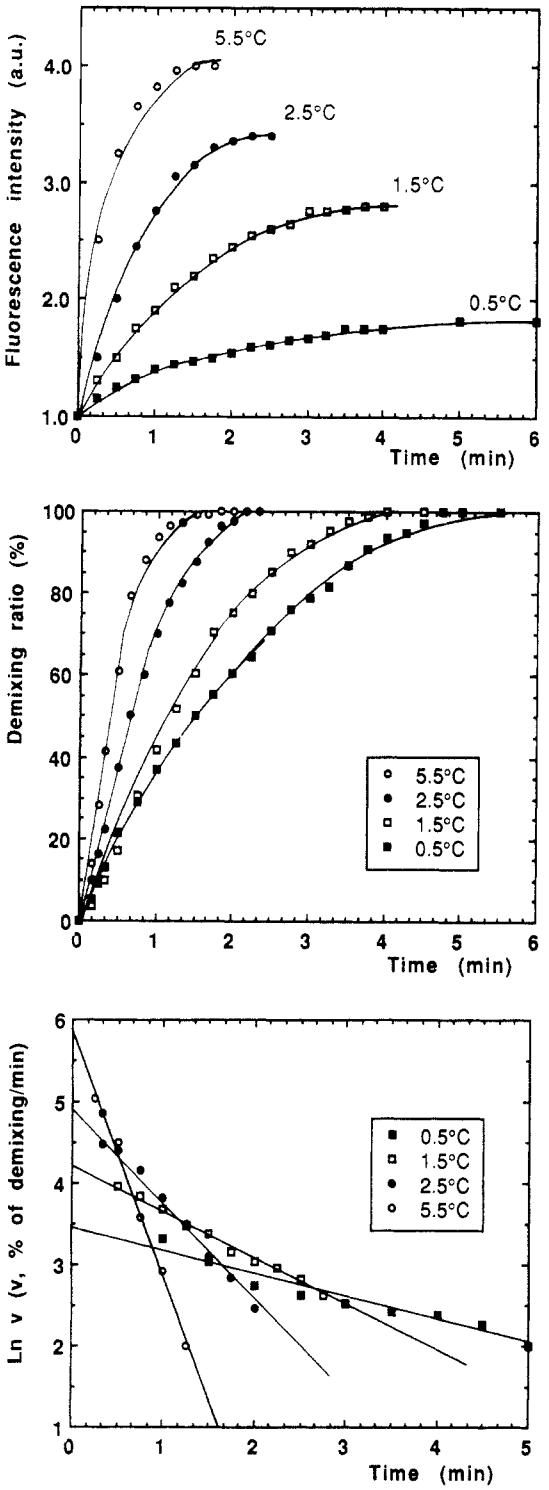

Figure 3. Example of the blend PVME/PS-HDH held in isothermal conditions at different depths at quench in the two-phase region: (a) fluorescence intensity *vs* time; (b) demixing ratio *vs* time; (c) rate of demixing *vs* time.

by comparison with the quantity $T_{cal\,1}$. This value can be calculated for the random hydrogenous–deuterated PS copolymer of similar composition, by assuming the validity of a mixing law of the form

$$T_{cal\,1} = 120\frac{n_H}{n_H + n_D} + 159\frac{n_D}{n_H + n_D}$$

In this equation, n_H and n_D represent the overall degrees of polymerization of the hydrogenous and deuterated monomers, respectively, and 120 and 159 °C are the LCST values in the presence of PSH and PS-d_8, respectively.[3]

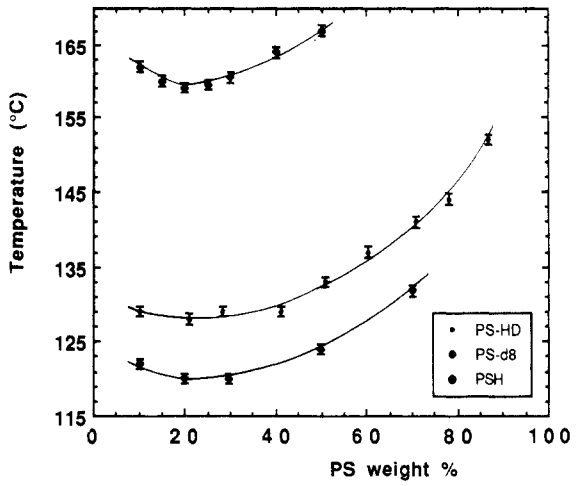

Figure 4. LCST phase diagram of the PVME/PS-HD blends. (Those for the blends PVME/PSH and PVME/PS-d_8 of identical polymer chain lengths are also given for comparison purposes.)

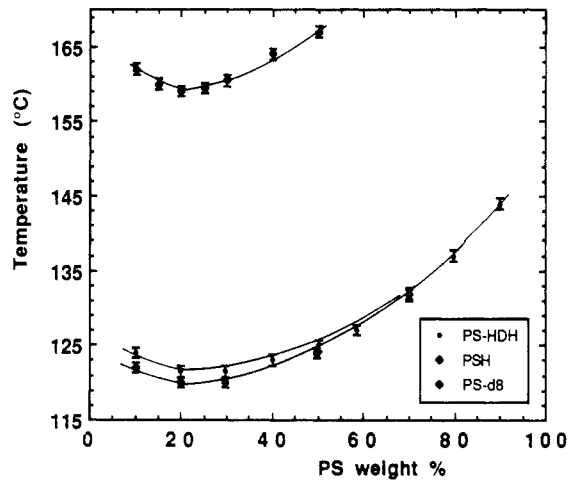

Figure 5. LCST phase diagram of the PVME/PS-HDH blends. (Those for the blends PVME/PSH and PVME/PS-d_8 of identical polymer chain lengths are also given for comparison purposes.)

Table 2. Values of the Phase Separation Temperatures, $T_{cal\,1}$ and $T_{cal\,2}$, Calculated from the Experimental Values Relative to PSH and PS-d_8

material	n_H	n_D	T_s(exp) (°C)	$T_{cal\,1}$ (°C)	$T_{cal\,2}$ (°C)
PSH	1775	0	120		
PS-d_8	0	1775	159		
PS-HD	1510	241	128	125.4	124.9
PS-HDH	1519	268	121.5	125.8	125.5

Use of a reciprocal-type mixing law of the form

$$\frac{1}{T_{cal\,2} + 273} = \frac{1}{393}\frac{n_H}{n_H + n_D} + \frac{1}{432}\frac{n_D}{n_H + n_D}$$

yields a value $T_{cal\,2}$ which is identical to $T_{cal\,1}$ within experimental error (Table 2). As also shown in Table 2, the LCST is higher in the presence of PS-HD than it would be on average ($T_{cal\,1}$ or $T_{cal\,2}$); however, it is lower in the presence of PS-HDH. In other words, PS-HD and PS-HDH exhibit shifts in opposite directions toward the calculated values. It is also worth noting that the observed shifts, although small, are greater than the error bars on the experimental determinations of the LCST's.

The influence of heating rate on the detection of phase separation in continuous heating conditions, that is, in ramp experiments, is illustrated in Figures 6a and 7 for PVME/PS-HD and PVME/PS-HDH blends, respectively. Such curves are similar to those previously reported in

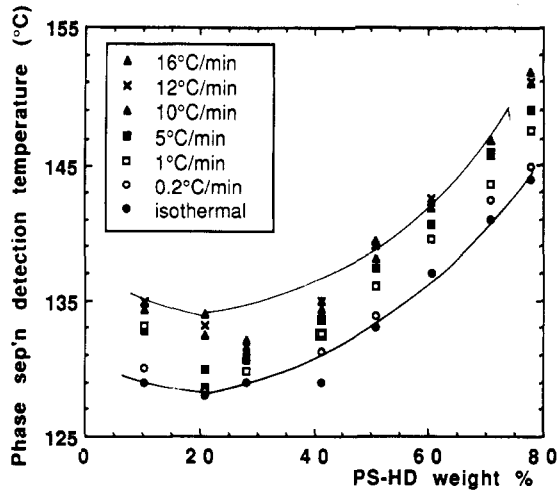

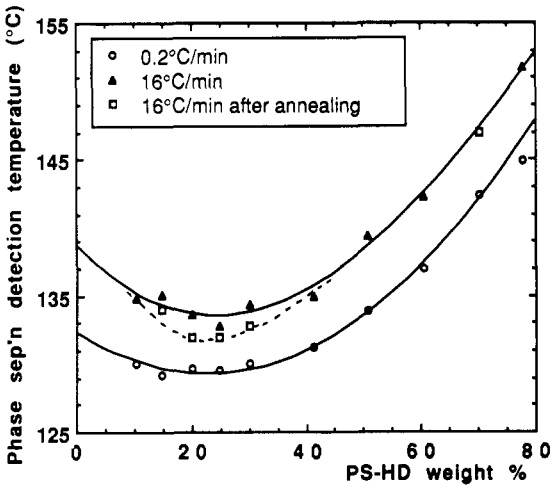

Figure 6. Effect of heating rate on the fluorimetric detection of phase separation in PVME/PS-HD blends: (a) as-prepared films; (b) films annealed for 2 h at 118 °C.

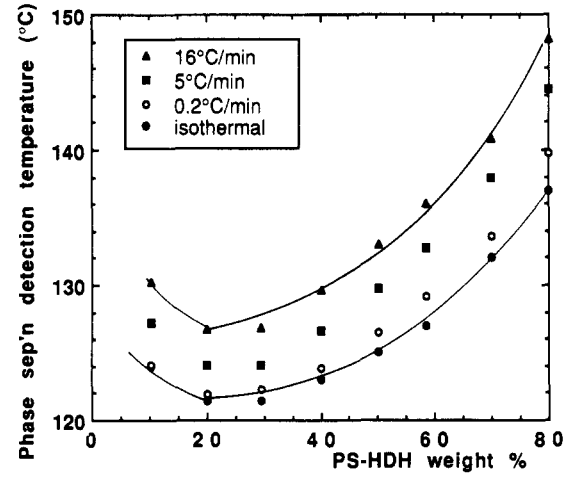

Figure 7. Effect of heating rate on the fluorimetric detection of phase separation in PVME/PS-HDH blends.

the literature for hydrogenous materials[2] and to that of the blend PVME/PSH shown in Figure 8. Their origin can be understood very simply, at least in the region of the minimum, where phase separation occurs by spinodal decomposition. From a thermodynamic viewpoint, spinodal decomposition is a spontaneous process, since the one-phase state is unstable. However, phase separation may still be a low-rate process because of the high viscosity of the medium when the molecular masses of the polymers are large enough (typically, more than 100 000). When

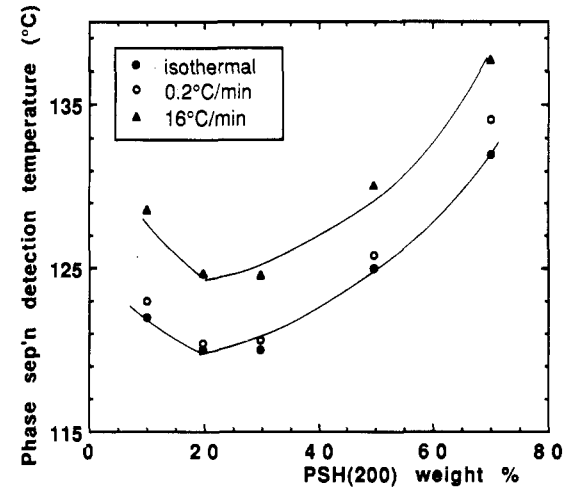

Figure 8. Effect of heating rate on the fluorimetric detection of phase separation in PVME/PSH blends.

Table 3. Heating Rate Effects on the Phase Separation Detection Temperature

	PVME/PSH	PVME/PS-HDH	PVME/PS-HD
T_{16}(min) (°C)	124.7 ± 0.5	126.7 ± 0.5	134.0 ± 0.5
T_{coex}(min) (°C)	120.0 ± 0.5	121.5 ± 0.5	128.0 ± 0.5
$100/\Delta T_{min}$	22.5 ± 5	20 ± 4	17 ± 3

Table 4. Values of the Initial Phase Decomposition Rates, v_0 (Percent of Demixing per Minute), at Different Depths of Quench, ΔT (°C)

ΔT	PVME/PSH	PVME/PS-HDH	PVME/PS-HD
0.5	33 ± 5	45 ± 4	99 ± 3
1.5	94 ± 5	74 ± 4	121 ± 3
2.5	155 ± 5	148 ± 4	164 ± 3
3.5	216 ± 5	200 ± 4	211 ± 3
4.5	274 ± 5	245 ± 4	270 ± 3
5.5	337 ± 5	315 ± 4	314 ± 3

this is the case, detection of phase separation is delayed to higher temperatures, especially when the heating rate exceeds the rate of spinodal decomposition at a given temperature.

This analysis, based on nonequilibrium conditions, is corroborated well by the results presented in Figure 6b. Indeed, phase separation in a sample annealed for 2 h at $T = (T_{coex} - 10\ °C)$ before a further heating ramp at 16 °C min^{-1} is detected at a temperature lower than that of the same sample continuously heated at 16 °C min^{-1} from room temperature. The reason for this is that the latter sample is farther from equilibrium at the temperature T_{coex} than the former.

Let T_{16}(min) and T_{coex}(min) be the temperatures at which the LCST is detected using a heating rate of 16 °C min^{-1} and isothermal conditions, respectively. Thus, the reciprocal of T_{16}(min) − T_{coex}(min), called $1/\Delta T_{min}$, is indicative of the rate of spinodal decomposition. As shown in Table 3, $1/\Delta T_{min}$ seems to depend on the degree of deuteration of the PS chain. However, since the observed differences are rather small with regard to the error bars on the measurements, direct determinations of phase separation rate are necessary. As detailed in the Experimental Section, the initial rates of phase separation, v_0, can be deduced from the experimental data relative to different depths of quench ΔT. The corresponding values are grouped in Table 4. In the earlier stages of spinodal decomposition, starting at the temperature $T_s = T_{coex}$(min), plots of v_0 versus $\Delta T/T_s$ are expected to be linear and to pass through the origin. This is satisfactorily verified by the blend PVME/PSH and by the PVME/PS block copolymer blends (Figure 9). Inspection of the slopes

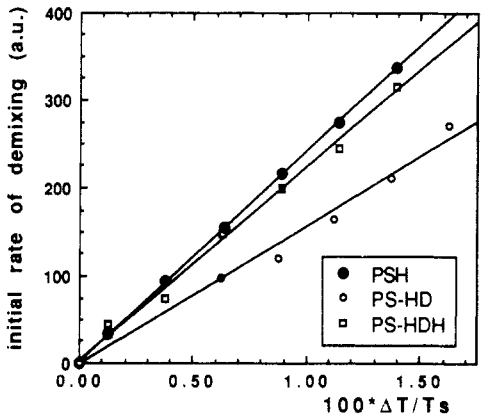

Figure 9. Spinodal decomposition initial rates versus $(T - T_s)/T_s$ for blends (80:20) of PVME with PSH, PS-HD, and PS-HDH.

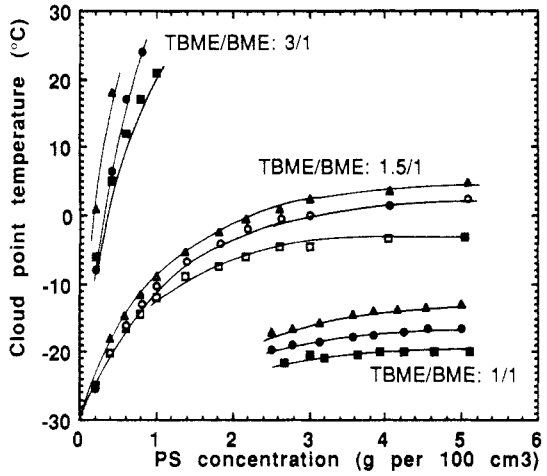

Figure 10. UCST phase diagrams of solutions of linear PS's in TBME/BME mixtures: squares, PS-HD; circles, PS-HDH; triangles, PSH.

indicates that the phase decomposition rates follow the sequence PSH > PS-HDH > PS-HD.

The credibility of these copolymer morphology effects is reinforced by the inspection of the UCST-type phase diagrams of solutions of the different PS's in monomeric analogs of PVME. Mixtures of *n*-butyl methyl ether (BME) and *tert*-butyl methyl ether (TBME) were used for this purpose. Indeed, solubility of the PS's in pure BME is too large for the UCST to be detected at a convenient temperature; on the other hand, solubility in pure TBME is not sufficiently high for the UCST to be detected well below the solvent boiling point. The phase diagrams relative to three different mixtures of BME and TBME and the polymers PSH, PS-HD, and PS-HDH are given in Figure 10. Clearly, TBME acts as a poorer solvent than BME. Indeed, the greater the TBME/BME ratio, the higher are the temperatures at which the one-phase domain is reached. For the TBME/BME ratios 1.5:1 and 1:1, the UCST is observed at a concentration roughly equal to 50 g L^{-1}. This value does not depend on the nature of the polymer, since all the materials under consideration exhibit the same chain length and polydispersity.

More instructive is the fact that the miscibility of any solvent mixture composition varies according to the sequence PSH < PS-HDH < PS-HD. This result is exactly symmetrical to what is deduced from the LCST data presented in figures 4 and 5: the higher the LCST in PVME blends, the lower is the UCST in small molecules which resemble the PVME subunit.

Star PS-Based Blends. Phase coexistence curves of the PVME/PS-$(DH)_6$ and PVME/PS-$(HD)_6$ blends are

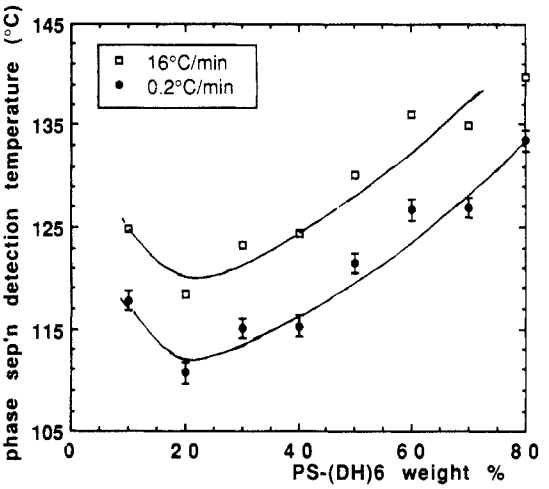

Figure 11. Effect of heating rate on the fluorimetric detection of phase separation in PVME/PS-$(DH)_6$ blends.

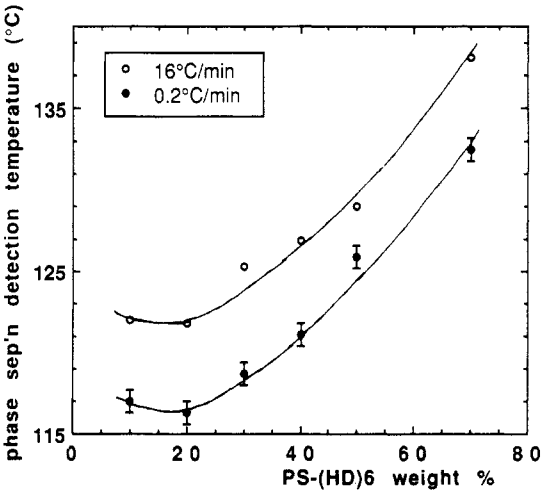

Figure 12. Effect of heating rate on the fluorimetric detection of phase separation in PVME/PS-$(HD)_6$ blends.

presented in Figures 11 and 12, respectively. Since only partly deuterated star materials are available at the moment, a full understanding of the effect of isotopic substitution on the miscibility window will have to await studies on the fully deuterated stars. This will be the subject of a future communication.

In the meantime, it is difficult to be sure that isotope substitution increases the miscibility window, as it does in the presence of linear PS's. At most, one may notice that the observed LCST values, that is, 111 and 116 °C, respectively, are both higher than that relative to a linear hydrogenous PS of identical overall chain length, which would be around 107 °C.[2]

The point of interest in the present paper is the influence on the miscibility of the position of the deuterated blocks, either in the core of the stars (PS-$(HD)_6$) or at the ends of their arms (PS-$(DH)_6$). The latter position leads to an increase in the LCST by 5 °C.

In the case of star PS's, no indication of the influence of copolymer morphology on phase separation kinetics can be derived from the inspection of $1/\Delta T_{min}$, calculated from Figures 11 and 12. Indeed, both values of ΔT_{min} are close to each other (about 10 °C) and have large error bars (±2 °C).

As shown in Figure 13, mixtures of PS-$(HD)_6$ with monomeric analogs of PVME exhibit a UCST at about −3 °C, which is lower than that observed in the presence of PS-$(DH)_6$ at about +2 °C. Thus, as in the case of linear polystyrene copolymers, LCST and UCST phase diagrams

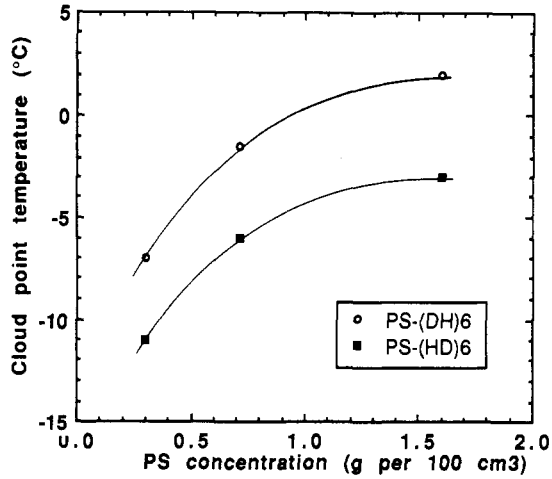

Figure 13. UCST phase diagrams of solutions of star PS's in the mixture TBME/BME (1:1.5).

are consistent with each other: when copolymer morphology effects lead to an increase in miscibility of the mixtures, both an increase of the LCST and a decrease of the UCST are observed.

Discussion

Although the data available for the star PS copolymers are incomplete at the moment, they are still easier to interpret than those of the linear copolymers. As a result of the star architecture, it is unquestionable that the deuterated segments of PS-$(DH)_6$, located in the core of the stars, are less accessible to the ether functions of PVME than the deuterated segments of PS-$(HD)_6$, located at the ends of the star arms. The same conclusion holds in solution about their relative accessibility to the ether functions of the solvent. Since earlier studies have clearly established that the occurrence of interactions between ether functions and deuterated phenyl rings is favorable to the miscibility,[3-5] it is reasonable to observe that the miscibility in the presence of PS-$(HD)_6$ is enhanced, as compared to what it is in the presence of PS-$(DH)_6$. As marked by an increase in LCST and a decrease of UCST of 5 °C each, these effects are weak because the relevant changes in the Flory interaction parameter are expected to be extremely small.[4]

In the same way, it is possible to interpret why the miscibilities in the presence of the diblock PS-HD are greater than those relative to the triblock PS-HDH, as revealed by an increase in the LCST of 6.5 °C and a decrease of the UCST of about 8 °C. Indeed, one may assume that the segmental concentration in the core of the macromolecular coils is much higher than that at their outer edges. Thus, the deuterated middle block of PS-HDH is likely to have comparatively less interaction with the ether functions of the small-molecule solvent (and, in the melt, with PVME as well) than the deuterated end block of PS-HD. Again, such effects are small and thus probably impossible to detect from direct interaction coefficient measurements.

Comparison of the spinodal decomposition rates in the melt, which were shown to follow the sequence v_0(PSH) > v_0(PS-HDH) > v_0(PS-HD), is consistent with this idea of accessibility-controlled interactions. Indeed, the values of phase separation rate are the result of a balance between two separate effects which go in opposite directions. First, the presence of stronger enthalpic interactions in the blend, marked by the effective occurrence of the PVME–PS deuterated phenyl ring interactions, leads to a decrease of the phase separation rate. Second, at a given ΔT, an increase in T_{coex} increases the displacement of the systems from their glass transition temperature, which is equal to -28 ± 0.5 °C for the three blends under consideration, and thus increases the chain mobility and the phase separation rate. As shown by earlier observations,[9] the latter effect would be the dominant factor in a comparison of the spinodal decomposition rates in the presence of either PSH or PS-d_8 as the result of the large difference in T_{coex} (39 °C). On the other hand, for the three systems being compared here, namely, PSH, PS-HDH, and PS-HD, the differences in their T_{coex} are rather small. Thus, the former effect overcomes the latter. As a consequence, the influence of accessibility-favored interactions on the phase separation kinetics is observed.

Conclusion

Study of the miscibility behavior of blends of PVME with hydrogenous-block-deuterated PS's of different architecture is an interesting route to the analysis of polymer–polymer interactions on a short-range scale. In spite of the small differences in behavior expected from the blends under consideration, suitable conclusions could be drawn due to the availability of carefully prepared and well-defined polymers and to the use of a very precise fluorimetric technique for the evaluation of phase separation. Our data corroborate the conclusions of earlier studies, showing that deuterium substitution on the PS's phenyl rings leads to a systematic increase in the LCST of the blends with PVME. In addition, they show a similar increase in solubility in solutions with monomeric analogs of PVME, as revealed by the decrease of UCST.

In addition, the small differences accompanying discrete changes in block characteristics such as the replacement of one hydrogenous block by two hydrogenous ones of length one-half are interpreted in terms of probability of accessibility of the ether groups to the thermodynamically favorable deuterated phenyl rings. These effects are shown to also affect the kinetics of spinodal decomposition.

Acknowledgment. We thank the French Ministry of Research and the Spanish Ministry of Education and Science for a fellowship grant to J.M.G.-E. in the context of the "Plan de Formacion del Personal Investigador".

References and Notes

(1) Halary, J. L.; Ubrich, J. M.; Nunzi, J. M.; Monnerie, L.; Stein, R. S. *Polymer* **1984**, *25*, 956.

(2) Ubrich, J. M.; Ben Cheikh Larbi, F.; Halary, J. L.; Monnerie, L.; Bauer, B. J.; Han, C. C. *Macromolecules* **1986**, *19*, 810.

(3) Ben Cheikh Larbi, F.; Leloup, S.; Halary, J. L.; Monnerie, L. *Polym. Commun.* **1986**, *27*, 23.

(4) Yang, H.; Hadziioannou, G.; Stein, R. S. *J. Polym. Sci., Polym. Phys. Ed.* **1983**, *21*, 159.

(5) Halary, J. L.; Ubrich, J. M.; Monnerie, L.; Yang, H.; Stein, R. S. *Polymer Commun.* **1985**, *26*, 73.

(6) Halary, J. L.; Monnerie, L. In *Photophysical and Photochemical Tools in Polymer Science*; Winnik, M., Ed.; D. Reidel: Dordrecht, 1986; p 589.

(7) Ben Cheikh Larbi, F.; Halary, J. L.; Monnerie, L. *Macromolecules* **1991**, *24*, 867.

(8) Lantman, C. W.; Tassin, J. F.; Monnerie, L.; Fetters, L. J.; Helfand, E.; Pearson, D. S. *Macromolecules* **1989**, *22*, 1184.

(9) Ben Cheikh Larbi, F. Ph.D. Thesis, Université Paris-Sud Orsay, 1987.